Author(s): Bennour, Ines; Haukka, Matti; Teixidor, Francesc; Viñas, Clara; Kabadou, Ahlem

Title: Crystal structure and Hirshfeld surface analysis of [N(CH3)4][2,2'-Fe(1,7-closo-C2B9H11)2]

Year: 2017

Version:

Graphical Abstract

The two red spots presented on the anionic and cationic HS presentations give an idea about the attendance of two different interactions H···H related the same proton, from the $[N(CH_3)_4]$ cation, with two different H-B vertex from the adjacent anion.
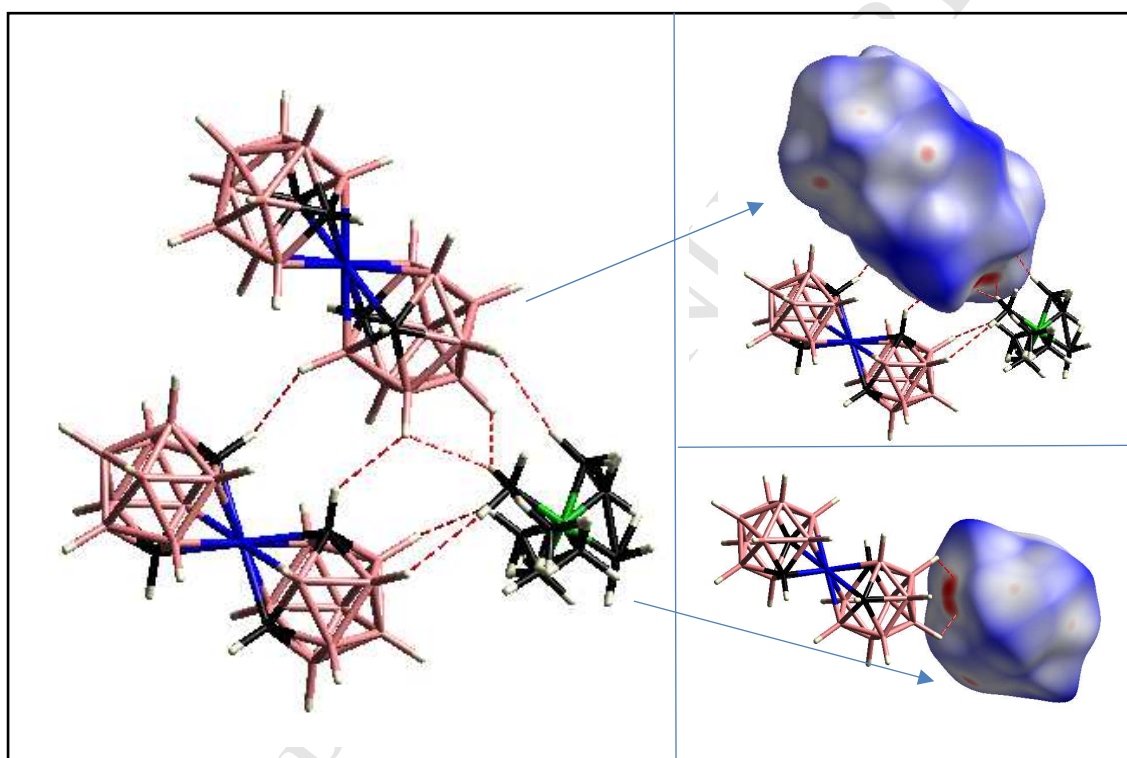
Crystal Structure and Hirshfeld Surface Analysis of [N(CH$_3$)$_4$][2,2'-Fe(1,7-*closo*-C$_2$B$_9$H$_{11}$)$_2$]

Ines Bennour,[a,b] Matti Haukka,[c] Francesc Teixidor,[b] Clara Viñas,[b,]* Ahlem Kabadou[a,]*

[a] Laboratoire de Sciences des Matériaux et de l'Environnement, Faculté des Sciences de Sfax, Université de Sfax, B.P. 1171, 3000 Sfax, Tunisie. E-mail: ahlemkabadou@yahoo.fr

[b] Institut de Ciència de Materials de Barcelona (ICMAB-CSIC), Campus U.A.B., 08193, Bellaterra, Barcelona, Spain. E-mail: clara@icmab.es

[c] Department of Chemistry, University of Jyväskylä, FIN-40014, Jyväskylä, Finland

ABSTRACT

This work investigates the *meta*-ferrabis(dicarbollide) anion that was isolated as salt of tetramethylammonium. The structure of the obtained crystal consisted of discrete [2,2'-Fe(1,7-*closo*-C$_2$B$_9$H$_{11}$)$_2$]$^-$ anions and disordered [N(CH$_3$)$_4$]$^+$ cations. The anion had a considerable chemical stability ensured by ionic and Van der Waals interactions. Thus, Hirshfeld surfaces and fingerprint plot were used to visualize, explore, and quantify intermolecular interactions in the crystal lattice of the title compound. This investigation proved that close contacts were dominated by H⋯H interactions.

Keyword: *meta*-carborane, metallabis(dicarbollide), Hirshfeld study, dihydrogen bonds.

1. INTRODUCTION

The study of new compounds formed when main group, *d*- and *f*-block metals are incorporated in multicage carborane compounds has attracted a great interest due to its high added value in several applications [1]. For this reason, the discovery of metallabis(dicarbollide) complexes by Hawthorne *et al.* (1965) has been of major importance for borane and organometallic chemistries till the present. The most known metallabis(dicarbollide) complexes are the ones whose general formula is $[3,3'-M(1,2-C_2B_9H_{11})_2]^-$[2]. These complexes consist of two η^5-carboranyl ligands, *nido*-$[7,8-C_2B_9H_{11}]^{2-}$, and an M^{3+} metal located in between. The η^5-carboranyl ligand possesses 6π electrons delocalized in the open pentagonal $[C_2B_3]^{2-}$ face similar to the metal-bonding orbitals of the cyclopentadienyl ligand $[C_5H_5]^-$. However, there are several differences between ferrocene and ferra(bisdicarbollide) complexes. In fact, ferrocene is neutral. The hydrogen atoms bonded to the carbons beam out of the center of the aromatic ring. Substituents are largely coplanar with the pentagonal C_5 ring and substituents can only be at one plane. Conversely, ferra(bisdicarbollide) is monoanionic where the hydrogen atoms beam out of the center of the icosahedron. The substituent can therefore be located at different planes and are noncoplanar with the pentagonal $[C_2B_3]^{2-}$ face.

The interest in these sandwich molecules emanates from the multiple properties that they possess. They have one negative charge distributed throughout the volume of the complex. They are electroactive compounds with a low charge density [3]. They show thermal and chemical stability [1a] and an amphiphilic character [4], as well. This richness explains the many attempts to suggest new metallabis(dicarbollide) derivatives applicable to materials science [5] as an electroactive species in sensors [6] and biosensors [7], as a doping agent in conducting organic polymers [1h], as an extractant of radionuclides from nuclear waste [8], in dye-sensitized solar cells [9] in medicine [10] and in several other fields.

2

The study of metallabis(dicarbollide) compounds has specially addressed the η^5-carboranyl ligand derivatives of *nido*-[7,8-$C_2B_9H_{11}$]$^{2-}$ but very little is reported on the η^5-carboranyl ligand of the isomer *nido*-[7,9-$C_2B_9H_{11}$]$^{2-}$ that contains the two carbon atoms located at the open [C_2B_3]$^{2-}$ face andseparated by one boron atom [11]. Additionally, a survey of the Cambridge Structural Database (CSD) [12] by means of ConQuest [13] on December 12th 2016, revealed fourteen crystal structures of substituted *meta*-metallabis(dicarbollide) [14] complexes, of which eleven are zwitterion complexes (Co (7 structures), Ni (2 structures), Cu and Fe) [15], two are monoanionic of Co^{3+} *meta*-metallabis(dicarbollide) [16] and one is dianionic with Ni^{2+} [17]. To our knowledge, there are no reported structures of non-substituted monoanionic sandwich *meta*-ferrabis(dicarbollide).

This work addresses the study of the crystal structure of [N(CH$_3$)$_4$][2,2'-Fe(1,7-*closo*-$C_2B_9H_{11}$)$_2$] synthesized by complexation reaction of *nido*-[7,9-$C_2B_9H_{11}$]$^{2-}$ with FeCl$_2$. In addition to solving the scarcity of crystal structures of plain [2,2'-Fe(1,7-*closo*-$C_2B_9H_{11}$)$_2$]$^-$, our aim was also to check whether the non-adjacent position of the two carbons in C_2B_3 face can influence the structure of the compound by altering the distance between the metal and centroids C_2B_3. We compared the present [2,2'-Fe-1,7-*closo*-($C_2B_9H_{11}$)$_2$]$^-$ and the common [3,3'-Fe-1,2-*closo*-($C_2B_9H_{11}$)$_2$]$^-$ anionic compound. This study is based on the results of monocrystal X-ray diffraction analyses of the complex [N(CH$_3$)$_4$][2,2'-Fe(1,7-*closo*-$C_2B_9H_{11}$)$_2$] and its Hirshfeld surface analysis.

2. EXPERIMENTAL SECTION

Synthesis of [N(CH$_3$)$_4$][2,2'-Fe(1,7-closo-C$_2$B$_9$H$_{11}$)$_2$]

To a stirring solution of [HN(CH$_3$)$_3$] [7,9-*nido*-$C_2B_9H_{12}$] [18] (100 mg, 0.517 mmol) at 0°C in dry THF (5 ml) under nitrogen, 0.78 ml of *n*-BuLi (1.55 mmol, 2M) was added dropwise. In another flask and under nitrogen, a suspension of FeCl$_2$ (196.7 mg, 1.55 mmol)

3

in THF (5 ml) was prepared. Then, the transparent solution of ligand was transferred to the suspension mixture and the reaction mixture stirred under reflux at inert atmosphere overnight. Then, the initially formed Fe(II) complex was converted to an Fe(III) compound by stirring the reaction solution for 2 h in the presence of air, and the solvent was then removed in vacuum. Extraction was carried out using 5 ml of diethyl ether and 5 ml of HCl (0.1 M). The organic phase was tried with $MgSO_4$, and after filtering, the solvent was evaporated and the obtained dark green solid dissolved in 3 ml of water and then precipitated using an aqueous solution of $[N(CH_3)_4]Cl$. The dark green solid that precipitated was collected and washed three times with water. Crystallization was done in benzene to give 160.56 mg of $[N(CH_3)_4][2,2'-Fe(1,7-closo-C_2B_9H_{11})_2]$ (Yield= 82 %). Elemental analysis: calc: C 24.33%, H 8.62%, N 3.55%; found: C 24.82%, H 9.44%, N 3.44%. ATR: ν = 3018 (C_c-H), 2899, 2836 (C-H$_{(methyl)}$), 2535 (w, B-H), 1477 (C-N) (Fig. S1). $^{13}C\{^1H\}$ NMR (d_6-acetone): δ= -55,18 (s, CH_3), -294.34 (C_c-H) (Fig. S2). $^{11}B\{^1H\}$-NMR (d_6-acetone): δ [ppm]= -400.9 (4B, B(6,11,6',11')), -321.9 (2B, B(3,3'), -22.4 (2B), 10.4 (4B), 26.6 (4B), 33.4 (2B) (Fig. S3). Maldi-TOF MS (%) =: m/z = 321.33 (100) (Fig. S4). Good green crystals suitable for X-ray diffraction were grown in acetone.

X-ray Structure Determination. The crystal of $[N(CH_3)_4][2,2'-Fe(1,7-closo-C_2B_9H_{11})_2]$ was immersed in cryo-oil, mounted in a Nylon loop, and measured at a temperature of 170 K. The X-ray diffraction data were collected on a Bruker Kappa Apex II diffractometer using Mo Kα radiation (λ = 0.710 73 Å). The *Denzo/Scapack* [19] program package was used for cell refinements and data reductions. The structure was solved by the charge flipping method using *SUPERFLIP* [20] software. A multiscan absorption correction based on equivalent reflections (*SADABS*) [21] was applied to the data. Structural refinement was carried out using the *SHELXL2016* [22] program. The Fe atom of $[N(CH_3)_4][2,2'-Fe(1,7-closo-C_2B_9H_{11})_2]$ was located on an inversion center. The carbon atoms of the NH_4^+ counter

cation were disordered over two sites around a two-fold rotation axis with equal occupancies. Due to this disorder, the N-C and C-C distances of the cation were restrained to be similar. Hydrogen atoms were positioned geometrically and constrained to ride on their parent atoms, with C-H = 0.98-1.12 Å, B-H = 1.12 Å, and U_{iso} = 1.2-1.5 U_{eq} (parent atom). The crystallographic details are summarized in Table 1. Crystallographic data (excluding structure factors) for the structures reported in this paper were submitted to the Cambridge Crystallographic Data Centre as supplementary publication no. CCDC 1527813. Copies of the data can be obtained free of charge from www.ccdc.cam.ac.uk/conts/retrieving.html.

The final anisotropic full matrix least squares refinement resulted in a convergence of the R factor at 0.046, Rw = 0.092. The crystal structures and packing interactions were depicted using Mercury [23] and DIAMOND [24], respectively.

Hirshfeld surface (HS) analysis

The Hirshfeld surface analyses were carried out using the CrystalExplorer program [25] which accepts a structure input file in the CIF format. HS analysis was performed to identify the types and regions of weak intermolecular interactions, and proportions of these interactions. Molecular HS in crystal structure was constructed from the electron distribution. Distance from the HS to the nearest nucleus inside and outside the surface was marked by the quantities d_i and d_e, respectively. d_{norm} is a normalized contact distance, which was defined in terms of d_i, d_e, and the Van der Waals radii of the atoms, as listed in equation (1):

$$d_{norm} = \frac{d_i - r_i^{vdW}}{r_i^{vdW}} + \frac{d_e - r_e^{vdW}}{r_e^{vdW}}$$

The combination of de and di in the form of 2D fingerprint plot provides an overview of intermolecular contacts in the crystal. The Hirshfeld surfaces mapped with a shape index range of −1.0 to 1.0 Å, d_{norm} range of −0.5 to 1.5 Å, and full fingerprint plot can be created.

3. RESULTS AND DISCUSSIONS

3.1. Crystal structure

Good crystals of $[N(CH_3)_4][2,2'-Fe(1,7-closo-C_2B_9H_{11})_2]$ suitable for X-ray-diffraction were grown from an acetone solution at -4ºC. The title compound was solved in a monoclinic system, C2/c space group with four formula units in unit cell (Z = 4) (Fig. S5). The Fe atoms lied on the 4(d) (1/4, 1/4, 1/2) sites, surrounded by four carbon atoms and six boron atoms in the same Wyckoff positions 8(f). The N atoms occupied the 4(e) (1/2, y, 1/4) sites, connected by four carbon atoms with 8(f) positions and the H atoms (by implication) the 8(f) (x, y, z) sites.

Noticeable is the packing of $[N(CH_3)_4][2,2'-Fe(1,7-closo-C_2B_9H_{11})_2]$ along the *c* axis, shown in Fig. S6, in which the anionic and cationic layers pack one on top of each other. The B/C assignments in the cage are well-established from B-C and B-B distances[26] and displacement ellipsoid behavior, and do not appear to be disordered. The asymmetric unit of the studied crystal consisted of half a $[2,2'-Fe(1,7-closo-C_2B_9H_{11})_2]^-$ anion (Fig. 1) located on an inversion center, and one half occupied $[N(CH_3)_4]^+$ cation disordered over a two-fold axis as displayed in Fig. S7. For one cation, the static disorder was a simple 50:50 split over two sites. Tetramethylammonium chloride was the salt used in this synthesis to produce the quaternary ammonium cation as a counterion. The methyl groups were tetrahedrally arranged around the central N atom. The 11-vertex polyhedral present in one cage of the anion part was formed of triangulated faces. In addition, in the anion part, the iron ion was coordinated by four carbon and six boron atoms (Fig. 2). The Fe atom was displayed as an inversion center between the two cages of *nido* C_2B_9 clusters. This central metal atom, in oxidation state (+III), is η^5 bonded to two dicarbollide ligands, each contributing with two negative charges. It was localized between the two open pentagonal faces C_2B_3 (Fig. 2b). The planar bonding faces of the two dicarbollide ligands in our compound were nearly parallel (Fig. 2a). Moreover, the

6

angles through the metal and between two opposite atoms (like C(1)-Fe-C(1)[a], a : 1/2-x, 1/2-y, 1-z) were 180°. The bond lengths at each planar pentagonal face were four B-C (1.698(3)-1.706(3) Å) and one B-B (1.792(3) Å). The three iron-boron interatomic distances were Fe-B(3): 2.100(2)Å, Fe-B(11): 2.131(2) Å, and Fe-B(6): 2.111(2) respectively, while the Fe-C_c distances average were 2.097Å.

3.2. H⋯H short interaction study

As shown by Fig. S8, each anion has self-interactions and anion-cation hydrogen interactions. There are eight possible self-interactions of the anion [2,2'-Fe(1,7-*closo*-$C_2B_9H_{11})_2$]$^-$ as presented in Fig. S8a The same figure demonstrates the presence of two different distances of the intermolecular bond H⋯H for the interactions C(1)-H⋯H-B and C(7)-H⋯H-B equal to 2.31 Å and 2.24 Å, respectively. This result is due to the fact that these interactions are related to (i) the acidic character of C_c⋯H where the proton has a positive charge and (i) the hydride character of the B-H vertex where the proton has a negative charge (according to Pauling scale for χ_H = 2.20, for the χ_B= 2.04 and for the χ_C= 2.55) [27]. On the other side, the two independent labeled ions are aggregated through 14 $C_{[N(CH3)4]+}$-H⋯H-B interactions by virtue of the donor character of the proton of [N(CH$_3$)$_4$]$^+$ in front of the acceptor character of the proton connected to the boron (Fig. S8b). C-H of six different disordered [N(CH$_3$)$_4$]$^+$ interact with the H-B of the center anion as follows: The two first [N(CH$_3$)$_4$]$^+$ molecules participated both with protons connected to C(3) and C(4) to produce H⋯H interactions equal to 2.25 Å and 2.35 Å, respectively. Although the other two cations participate with the same carbons (C(3) and C(4)), the distance of C(3)-H⋯H-B becomes longer (2.37 Å). On the other hand, the two remaining [N(CH$_3$)$_4$]$^+$ cations participate by different C-H vertex. The first one is the C(6)-H; where it presents H⋯H equal to 2.39 Å for both different [N(CH$_3$)$_4$]$^+$ cations. The second proton that is connected to C(5) presents a very

different behavior, and it interacts at the same time with two H-B from different vertices which present distances C(5)-H⋯H-B(1)= 2.24Å and C(5)-H⋯H-B(2)= 2.32Å.

3.3. Hirshfeld surface (HS) study:

In addition to the electrostatic contribution, the existing intermolecular C-H⋯H-B interactions also have an important role in the stabilization of this molecule. This was studied and confirmed by Hirshfeld surfaces (HS) analysis using the crystal explorer program. The HS can present the d_{norm} figure type in which contacts with distances equal to the value of Van der Waals radii are represented by a white color, and the contact distance with shorter values than Van der Waals are revealed by the red color, while the distances longer than Van der Waals are presented as blue color [28]. Also, the HS illustrated in the shape index figure reveals the character of proton present in each unity; the red concavity is related to the presence of an acceptor proton, while the blue convexity is related to the presence of a donor proton.

d_{norm}, shape index and 2-Dfingerprint plot figures of the $[N(CH_3)_4]^+$ cation and the $[2,2'-Fe(1,7-closo-C_2B_9H_{11})_2]^-$ anion are presented in Fig. 3. For the cation part, to generate HS, the two orientations with them partial occupancies are included. The molecular HS of anion and cation unity in $[N(CH_3)_4][2,2'-Fe(1,7-closo-C_2B_9H_{11})_2]$ structure is mapped over a d_{norm} range from -0.196 to 1.246 Å and -0.195 to 1.335 Å, respectively. Visual inspection of fingerprint plots reveals that the anion and cation have nearly the different fingerprint plots evince in the distribution of interaction (related *de* and *di* values) of the ions in asymmetric unit. The diffuse blue region manifested as a scattered point in the fingerprint plot is related to H⋯H contacts, which account for 100% of the total Hirshfeld surface area of each $[N(CH_3)_4][2,2'-Fe(1,7-closo-C_2B_9H_{11})_2]$ unity where $[N(CH_3)_4]^+$ and $[2,2'-Fe(1,7-closo-C_2B_9H_{11})_2]^-$ show a shorter H...H interaction. The shortest close contacts between hydrogen atoms have a distance of approximately 2.43Å (notice that the Van der Waals radium for the

hydrogen atoms is 1.2 Å). For $[2,2'-Fe(1,7-closo-C_2B_9H_{11})_2]^-$, complementary regions are visible in the 2-D fingerprint plots where one anion acts as a donor ($de<di$) and the other as an acceptor ($de>di$) [29]. Therefore, the 2-D fingerprint plots of cation $[N(CH_3)_4]^+$ had an asymmetric distribution in de and di; which indicates that the cation protons displayed a donor character ($de<di$).

The d_{norm} (normalized contact distance, see Equation1) surfaces reveal the close contacts of hydrogen bond donors and acceptors, and other contacts. The d_{norm} mapped on HS for visualizing the intermolecular interactions in the crystal lattice of $[N(CH_3)_4]^+$ and $[2,2'-Fe(1,7-closo-C_2B_9H_{11})_2]^-$ is shown in Fig. 3a and Fig. 3c, respectively. It demonstrates that the large circular depressions are visible on the front and back views of the surface of both analyzed unities with two forms: (i) convex form as labeled (1) and (4) relative to acceptor interaction C-H···H and (ii) convex form indexed as (3) characterizes donor B-H···H interaction in the structure. The H···H interactions are also evidenced in shape index by a red concave region around the acceptor hydrogen atom (labeled as (5) in Fig. 3e) that confirms the hydride character of the hydrogen connected to the Boron in cluster anion. Fig. 3b and 3e present a complementary blue convex region around the donor hydrogen atoms (indexed as 2 and 6, respectively); which is a consequence of the acidic character of C-H characterizing the $C_{[N(CH3)4]+}$-H···H and C_c-H···H interactions.

The two red spots on the HS presentations in Fig. 3a and Fig. 3b show the attendance of two different interactions H···H related to the same proton, from the $[N(CH_3)_4]^+$ cation, with two different H-B vertex from the adjacent anion. This explains the orientation of ions in the cell as confirmed by Fig. 4.

3.4. Comparison

The crystal structure of the dianionic *ortho*-ferrabis(dicarbollide) complex was synthesized by Hawthorne *et al.*[30]. A comparison of the dianionic [3,3'-Fe(1,2-*closo*-

$C_2B_9H_{11})_2]^-$ with the new monoanionic $[2,2'-Fe(1,7-closo-C_2B_9H_{11})_2]^-$ reported in this paper was made to check the influence of the position of carbon atoms as well as the charge in the crystals. In fact, both ferrabis(dicarbollide) isomers crystallize in the same unit cell with different space group as present in Table 2. In both structures, the presence of a disordered salt molecule in the crystal structures was observed, knowing that the tetramethylammonium is the cation in both compounds. Consequently, both isomers keep the same distance between the iron atom and the two pentagonal faces, but the volume of this space in *meta*-ferrabis(dicarbollide) compound was slightly increased. This small difference was observed through a small shift of values of Fe-C and Fe-B distances as presented in Table 3. The η^5-coordinate and the electronic factors made the iron similarly distant between the two opposite *nido*-carborane cages.

The synthesis of metallabis(dicarbollides) using the iron as a metal with carbons separated by one boron atom increases the stability of this ferrabis(dicarbollide) by a thermal factor.

CONCLUSIONS

The first crystal structures of plain $[2,2'-Fe(1,7-closo-C_2B_9H_{11})_2]^-$ anion where the two carbons of the face in C_2B_3 are in non-adjacent positions was reported as tetramethylammonium salt. The structure of the new crystal consisted of discrete $[2,2'-Fe(1,7-closo-C_2B_9H_{11})_2]^-$ anions and disordered $[N(CH_3)_4]^+$ cations. The ferrabis(dicarbollide) complexes of both isomers, $[N(CH_3)_4][3,3'-Fe(1,2-closo-C_2B_9H_{11})_2]$ and $[N(CH_3)_4][2,2'-Fe(1,7-closo-C_2B_9H_{11})_2]$, crystallize in the monoclinic system but in different space groups, $P2_1/C$ and $C2/C$, respectively. Hirshfeld surface studies were done for $[N(CH_3)_4][2,2'-Fe(1,7-closo-C_2B_9H_{11})_2]$ complex. The crystallographic structure of the anionic $[2,2'-Fe(1,7-closo-C_2B_9H_{11})_2]^-$ clusters was ensured by ionic and H···H short interaction.

Thus, Hirshfeld surfaces and fingerprint plot were used to visualize, explore, and quantify intermolecular interactions in the crystal lattice of the title compound. This investigation proved that close contacts were also dominated by H⋯H interactions.

REFERENCES

[1] a) J. Plesek, Chem. Rev. 92 (1992) 269-278; b) R.N. Grimes in *Carboranes*, Carboranes, 3rd Ed., Elsevier Inc. 2016; c) R. N. Grimes, J. Organomet. Chem. 747 (2013) 4-15; d) S.V. Timofeev, I.B. Sivaev, E.A. Prikaznova, V.I. Bregadze, J. Organomet. Chem. 751 (2014) 221-250; e) L. Deng, Z.W. Xie, Coord. Chem. Rev. 251 (2007) 2452-2476; f) I.B. Sivaev, V.I. Bregadze, J. Organomet. Chem. 614 (2000) 27-36; g) I.B. Sivaev, V.I. Bregadze, Collect. Czech. Chem. Commun. 64(5), (1999), 783-805. h) R. Núñez. I. Romero, F. Teixidor, C. Viñas, Chem. Soc. Rev. 45 (2016) 5147-5173; i) J. Cabrera-González, V. Sánchez-Arderiu, C. Viñas, T. Parella, F. Teixidor, R. Núñez, Inorg. Chem. 55 (2016) 11630−11634; j) N.S. Hosmane, J.A. Maguire, Comprehensive Organometallic Chemistry III, 3th Ed., 2007, 175-264; k) H.W. Roesky, S. Singh, K.K.M. Yusuff, J. A. Maguire, N.S. Hosmane, Chem. Rev. 106(9) *(*2006*)* 3813–3843.

[2] M.F. Hawthorne, T.D. Andrews, Chem. Commun. 19 (1965) 443-444.

[3] C. Masalles, J. Llop, C. Viñas, F. Teixidor, Adv. Mater. 14(11) (2002) 826-829.

[4] a) R.N. Grimes, Advanced Inorganic Chemistry, 6th Ed., 1999, 143; b) P. Bauduin, S. Prevost, P. Farras, F. Teixidor, O. Diat, T. Zemb, Angew. Chem. Int. Ed. 50 (2011) 5298-5300; c) M. Uchman, V. Dordovi, Z. Tosner, M. Pavel, Angew. Chem. Int. Ed. 54 (2015) 14113-14117.

[5] a) M.F. Hawthorne, J.I. Zink, J.M. Skelton, M.J. Bayer, C. Liu, E. Livshits, R. Baer, D. Neuhauser, Am. Assoc. Adv. Sci. Pub. 303 (2004) 1849; b) A. K. Singh, A. Sadrzadeh, B.I. Yakobson, J. Amer. Chem. Soc. 132(40) (2010) 14126-14129; c) J. Zhang, Z. Xie, Acc. Chem. Res. 47(5) (2014) 1623-1633; d) S.M. Gao, N.S. Hosmane, Russ. Chem. Bull. 63(4) (2014) 788-810; e) C. Viñas, F. Teixidor, R. Nuñez, Inorg. Chim. Acta. 409 (2014) 12-25.

[6] a) A.L. Stoica, C. Viñas, F. Teixidor, Chem. Commun. (2008) 6492–6494; b) A. L. Stoica, C. Viñas, F. Teixidor, Chem. Commun. (2009) 4988–4990.

[7] a) T. Garcia-Mendiola, V. Bayon-Pizarro, A. Zaulet, I. Fuentes, F. Pariente, F. Teixidor, C. Viñas, E. Lorenzo, Chem. Sci. 7 (2016) 5786-5797; b) I. Grabowska, A. Stachyra, A. Gora-Sochacka, A. Sirko, A.B. Olejniczak, Z.J. Lesnikowski, J. Radecki, H. Radecka, Biosens Bioelectron. 51 (2014) 170-176; c) R. Ziolkowski, A.B. Olejniczak, L. Gorski, J. Janusik, Z.J. Lesnikowski, E. Malinowska, Bioelectrochemistry. 87 (2012) 78-83.

[8] a) C. Viñas, S. Gómez, J. Bertrán, F. Teixidor, J. Dozol, H. Rouquette, Chem. Commun. (1998), 191–192; b) C. Viñas, S. Gómez, J. Bertrán, F. Teixidor, J. Dozol, H. Rouquette, Inorg. Chem. 37 (1998) 3640–3643; c) B. Grüner, J. Plesek, J. Báca, I. Cisarová, J. Dozol, H. Rouquette, C. Viñas, P. Selucký, J. Rais, New J. Chem. 26 (2002) 1519–1527; d) M. Bubenikova, P. Selucky, J. Rais, B. Gruner, P. Svec, J. Radioanal. Nucl. Chem. 293 (2012) 403-408. e) B. Gruner, P. Svec, Z. Hajkova, I. Cisarova, J. Pokorna, J. Konvalinka, Pure Appl. Chem. 84 (2012) 2243-2262.

[9] T.C. Li, A.M. Spokoyny, C. She, O.K. Farha, C.A. Mirkin, T.J. Marks, J.T. Hupp J. Am. Chem. Soc. 132 (2010) 4580-4582.

[10] a) Z. Lesnikowski, J. Med. Chem. 59(17) (2016) 7738-7758; b) M. Scholz, E. Hey-Hawkins, Chem. Rev. 111(11) (2011) 7035-7062; c) P. Cígler, M. Kožíšek, P. Řezáčová, J. Brynda, Z. Otwinowski, J. Pokorná, J. Plešek, B. Grüner, L. Dolečková-Marešová, M. Máša, J. Sedláček, J. Bodem, H. G. Kräusslich, V. Král, J. Konvalinka, Proc. Natl. Acad. Sci. U.S.A. 102(43) (2005) 15394-15399; e) J. F. Valliant, K. J. Guenther, A. S. King, P. Morel, P. Schaffer, O. O. Sogbein, K. A. Stephenson, Coord. Chem. Rev. 232(1-2) (2002) 173-230.

[11] V.L. Shirokii, A.A. Erdman, Z.P. Zubreichuk, N.A. Maier, Y.A. Oldekop, Zh. Obshch. Khim+. 53(4) (1983) 951-952.

[12] a) CSD version 5.38, November 2016 updates; b) J. Bruno, J.C. Cole, P.R. Edgington, M. Kessler, C.F. Macrae, P.M. Cabe, J. Pearson, R. Taylor, Acta Crystallogr. B58 (2002) 389-397.

[13] F.H. Allen, Acta Crys. B 58 (2002) 380.

[14] BOGQIX, ETCBNI, PUGRUE, PUGSAL, RAGPOE, RUJNEP, RUJNIT, VETLOV, VETLOV10, YAHLIC, YAHLOI, YAHLUO, YAHMAU, YAHMEZ.

[15] a) B. Grüner, I. Cisarová, A. Franken, J. Plešek, Tetrahedron: Asymmetry. (1998) 79–88; b) J. Plešek, A. Franken, R. Fröhlich, Collect. Czech. Chem. Commun. 62 (1997) 1070-1079; c) M.F. Hawthorne, A. Varadarajan, C.B. Knobler, S. Chakrabarti, R.J. Paxton, B.G. Beatty, F.L. Curtis, J. Am. Chem. Soc. 112 (1990) 5365-5366; d) A. Varadarajan, S. E. Johnson, F. A. Gomez,.S. Chakrabarti, C. B. Knobler, M. F. Hawthorne, J. Am. Chem. Soc. 114 (1992) 9003-9011.

[16] a) C. Viñas, S. Gomez, J. Bertran, J. Barron, F. Teixidor, J.F. Dozol, H. Rouquette, R. Kivekäs, R. Sillanpää, J. Organomet. Chem. 581 (1999) 188-193; b) J. Plešek, A. Franken, R. Fröhlich, Collect. Czech. Chem. Commun. 62 (1997) 57-61.

[17] R.M. Wing, J. Am. Chem. Soc. 92 (5) (1970) 1187–1190.

[18] M.F. Hawthorne, D. C. Young, P. M. Garrett, D. A. Owen, S. G. Schwerin, F. N. Tebbe, P. A. Wegner, J. Am. Chem. Soc. 90(4) (1968) 862-868.

[19] a) Z. Otwinowski, W. Minor, *Processing of X-ray Diffraction Data Collected in Oscillation Mode*, Academic Press, New York, pp. 307-326, 1997; b) In *Methods in Enzymology*, Volume 276, Macromolecular Crystallography, Part A, Carter, C. W., Sweet, J., Eds.; Academic Press: New York, USA, 1997; pp 307-326.

[20] L. Palatinus, G. Chapuis, J. Appl. Cryst. 40 (2007) 786-790.

[21] G. M. Sheldrick, *SADABS - Bruker Nonius scaling and absorption correction -,* Bruker AXS, Inc.: Madison, Wisconsin, USA, 2012.

[22] G. M. Sheldrick, Acta Cryst. (2015) C71, 3-8.

[23] C.E. Macrae, I.J. Bruno, J.A. Chisholm, P.R. Edgington, P. McCabe, E.Pidcock, L. Rodriguez-Monge, R.Taylor, J. Van de Streek, P. A. Wood, J. Appl. Cryst. 41 (2008) 466-470.

[24] K. Brandenburg, Diamond Version2.0 Impact Gbr, Bonn, Germany, 1998.

[25] S.K. Wolff, D.J. Grimwood, J.J.McKinnon, D. Jayatilaka, M.A. Spackamn, Crystal explorer 3.0, University of Western Australia, Perth, 2007.

26 A. McAnaw, G. Scott, L. Elrick, G.M. Rosair, A. J. Welch, Dalton Trans. 42 (2013) 645-664.

[27] E.J. Juarez-Perez, R. Nuñez, C. Viñas, R. Sillanpää, F. Teixidor, Eur. J. Inorg. Chem. (2010) 2385-2392.

[28] M. A. Spackman, D. Jayatilaka, Cryst. Eng. Commun. 11 (2009) 19–32.

[29] S. K. Seth, G. ChMaity, T. Kar, J. Mol Struct. 1000 (2011) 120–126.

[30] H.C. Kang, S.S. Lee, C.B. Knobler, M.F. Hawthorne, Inorg. Chem. 30 (1991) 2024-2031.

TABLES CAPTION

Table 1. Crystal data and structure refinement for $C_8H_{34}B_{18}FeN$.

Table 2. Details of the crystallographic data collection for dianionic *ortho* ferrabis(dicarbollide) and monoanionic *meta* ferrabis(dicarbollide) ligands.

Table 3. Selected Interatomic Distances (Å) between Fe-C and Fe-B obtained in ferrabis(dicarbollide) anions.

FIGURE CAPTIONS

Figure 1. The molecular and crystal structure of $[2,2'-Fe(1,7-closo-C_2B_9H_{11})_2]^-$ showing the atom numbering and displacement. Ellipsoids are at 50% probability level.

Figure 2. A view of the iron environment in $[N(CH_3)_4][2,2'-Fe(1,7-closo-C_2B_9H_{11})_2]$ (a) a 3D structure(b) a projection planar.

Figure 3. The *dnorm* and shape index Hirshfeld surfaces and the fingerprint plots of the anion and cation in $[N(CH_3)_4][2,2'-Fe(1,7-closo-C_2B_9H_{11})_2]$ crystal.

Figure 4. HS characterization of different H-B vertex from adjacent anion and cation.

Table 1.

Empirical formula	$C_8H_{34}B_{18}FeN$	
Formula weight	394.79	
Temperature	170(2) K	
Wavelength	0.71073 Å	
Crystal system	Monoclinic	
Space group	C2/c	
Unit cell dimensions	a = 22.7723(7) Å	α= 90°
	b = 10.1834(5) Å	β= 105.061(2)°
	c = 9.9464(5) Å	γ = 90°.
Volume	2227.3(2) Å^3	
Z	4	
ρ_{cal} (Mg/m^3)	1.177	
Absorption coefficient (mm^{-1})	0.672	
F(000)	820	
Crystal size	0.205 x 0.181 x 0.037 mm^3	
Theta range for data collection	2.204° to 29.167°.	
Index ranges	-31≤h≤29, -13≤k≤13,	
	-13≤l≤13	
Independent reflections	2991	
Absorption correction	Semi-empirical from equivalents	
Max. and min. transmission	0.7458 and 0.6759	
Refinement method	Full-matrix least-squares on F^2	
R_2 int	0.0492	
Final R indices [I>2sigma(I)]	R1[a] = 0.0466, wR2[b] = 0.0923	

[a] $R1 = \Sigma||F_o| - |F_c||/\Sigma|F_o|$. [b] $wR2 = [\Sigma[w(F_o^2 - F_c^2)^2]/ \Sigma[w(F_o^2)^2]]^{1/2}$.

Table 2 :

Chemical Formula	$C_{12}H_{46}FeB_{18}N_2$	$C_8H_{34}B_{18}FeN$
Radiation		Mo Kα
Wavelength/ Å		0.7107 Å
Isomer	*Ortho*	*meta*
Ref	[30]	our work
Solvent	$CH_3CN/(C_2H_5)_2O$	$(CH_3)_2CO$
Space group	$P2_1/c$	C2/c
a/ Å	9.017 (3)	22.772 (7)
b/ Å	11.341 (3)	10.183 (5)
c/ Å	32.941 (11)	9.946 (5)
β (°)	91.80 (1)	105.06
v/ Å^3	1381	2227(17)
Z	2	4
R	0.094	0.046
Rw	0.104	0.092
ρ(cal)/g cm^{-3}	1.13	1.17

Table 3.

Fe(2,2')-1,7-$(C_2B_{10}H_{11})_2$		Fe(3,3')-1,2-$(C_2B_{10}H_{11})_2$	
Fe(2,2^a)-C(1)	2.083(2)	Fe(3,3a)-C(1)	2.015 (8)
Fe(2,2^a)-C(1^a)	2.083(2)	Fe(3,3^a)-C(1 ^{a})	2.015 (8)
Fe(2,2^a)-B(3)	2.100(2)	Fe(3,3^a)-C(2)	2.047 (8)
Fe(2,2^a)-B(3^a)	2.100(2)	Fe(3,3^a)-C(2 ^{a})	2.047 (8)
Fe(2,2^a)-B(6)	2.111(2)	Fe(3,3^a)-B(4)	2.073(10)
Fe(2,2^a)-B(6^a)	2.111(2)	Fe(3,3^a)-B(4 ^{a})	2.073(10)
Fe(2,2^a)-C(7)	2.111(2)	Fe(3,3^a)-B(8)	2.144 (10)
Fe(2,2^a)-C(7^a)	2.111(2)	Fe(3,3^a)-B(8^a)	2.144 (10)
Fe(2,2^a)-B(11)	2.131(2)	Fe(3,3^a)-B(7)	2.112 (10)
Fe(2,2^a)-B(11^a)	2.131(2)	Fe(3,3^a)-B(7^a)	2.112 (10)
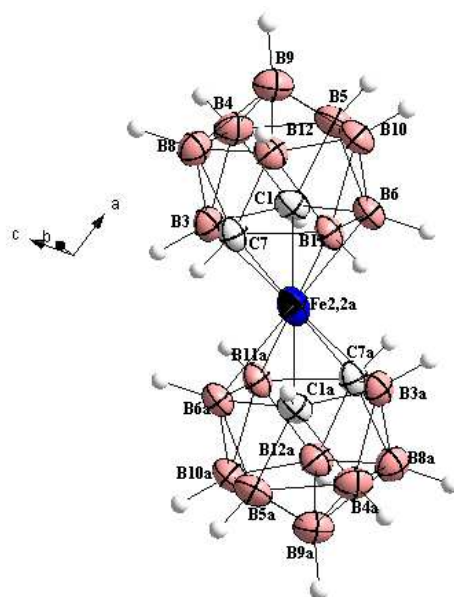
Figure 1:

Symmetry code :

a: 1/2-x, 1/2-y, 1-z

(a)   (b)

Figure 2:

$[N(CH_3)_4]^+$

(a)

d_{norm}

(1)

(c)

d_e

2.8
2.6
2.4
2.2
2.0
1.8
1.6
1.4
1.2
1.0
0.8
0.6

All interactions : H…..H (100%)

d_i

0.6 0.8 1.0 1.2 1.4 1.6 1.8 2.0 2.2 2.4 2.6 2.8

(b)

shape index

(2)

$[2,2'\text{-}Fe(1,7\text{-}closo\text{-}C_2B_9H_{11})_2]^-$

(d)

d_{norm}

(3)

(4)

(f)

d_e

2.8
2.6
2.4
2.2
2.0
1.8
1.6
1.4
1.2
1.0
0.8
0.6

All interactions : H…..H (100%)

d_i

0.6 0.8 1.0 1.2 1.4 1.6 1.8 2.0 2.2 2.4 2.6 2.8

(e)

*shape index*

(5)

(6)
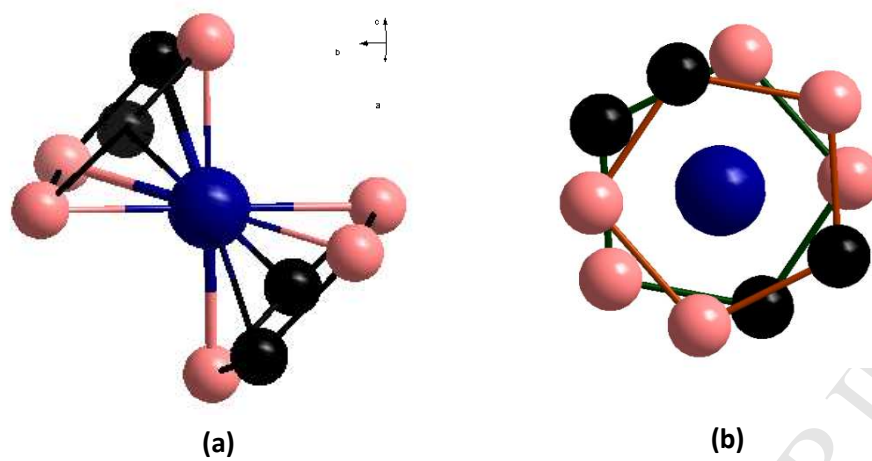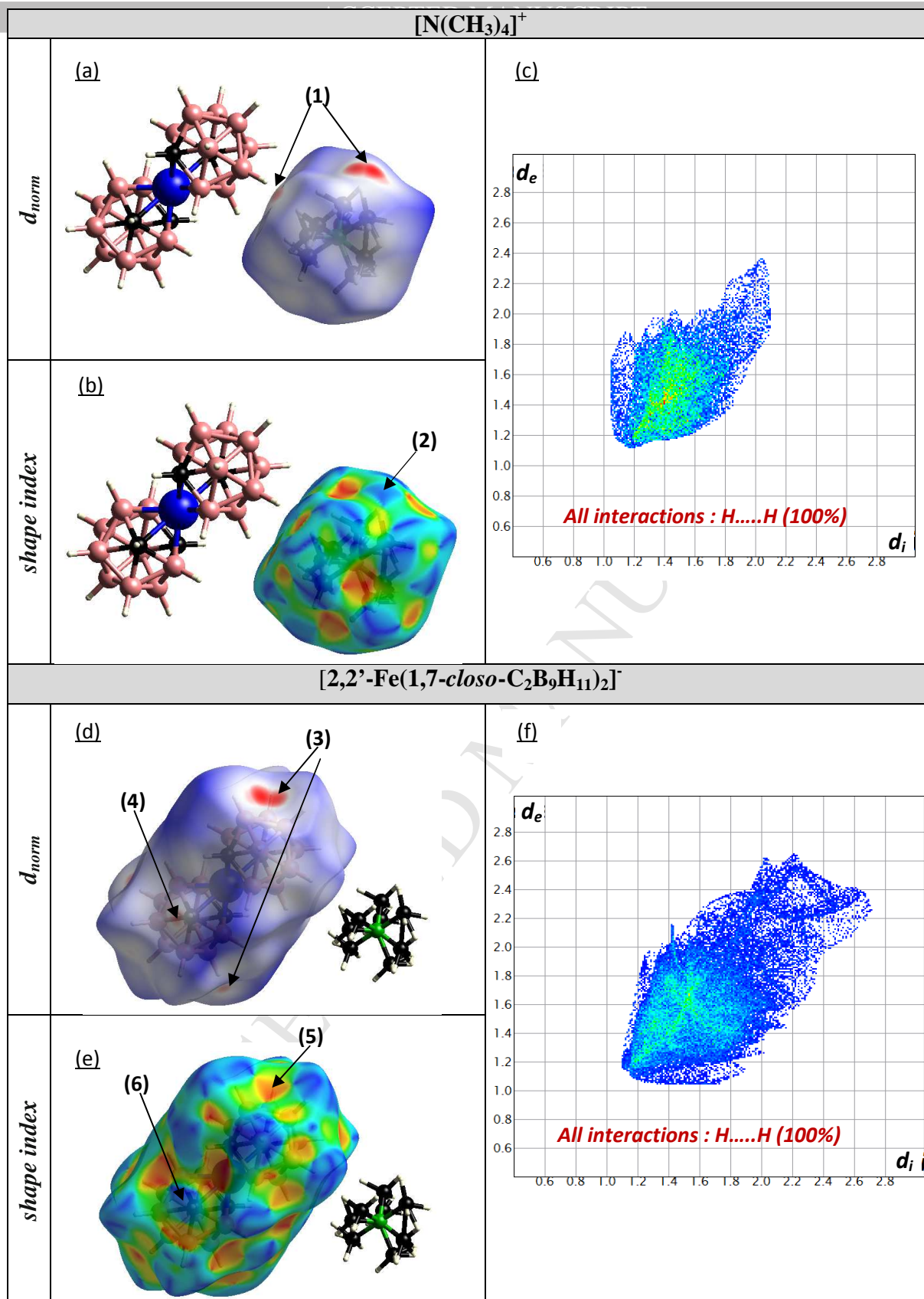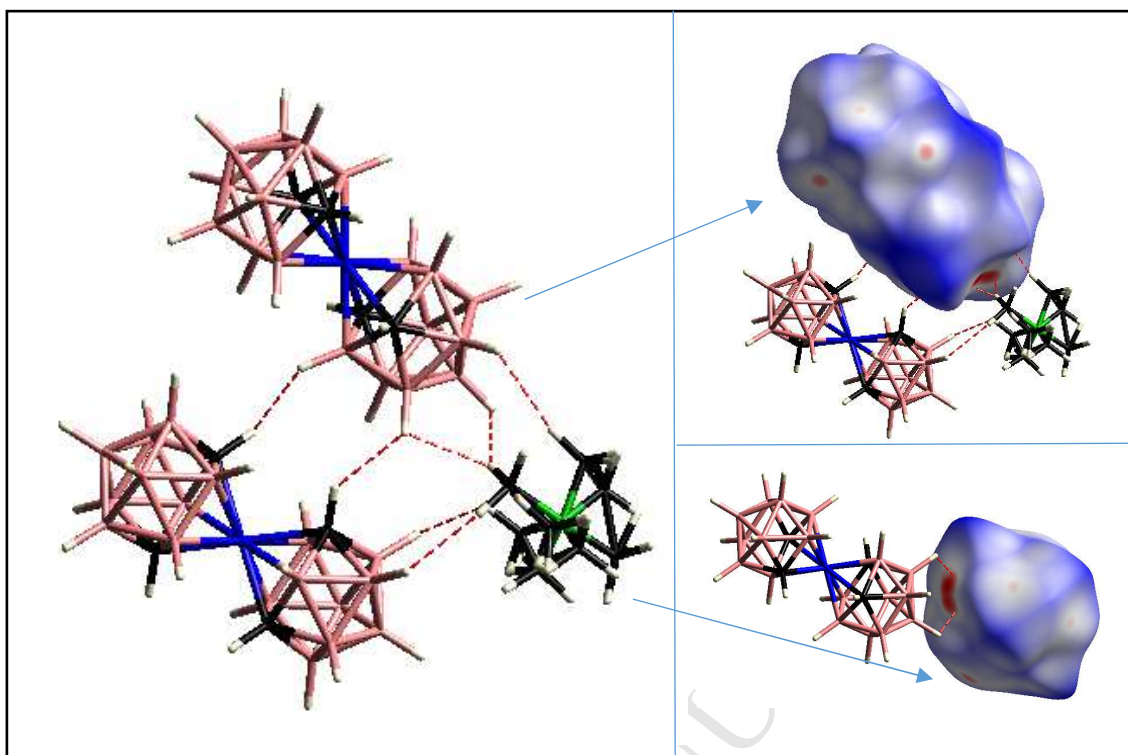
Figure 3.

Figure 4.

Highlights

- The [N(CH$_3$)$_4$] [2,2'-Fe(1,7-*closo*-C$_2$B$_9$H$_{11}$)$_2$] crystal was solved in a monoclinic system with C2/c space group.

- The structure of the obtained crystal consisted of discrete [2,2'-Fe(1,7-*closo*-C$_2$B$_9$H$_{11}$)$_2$]$^-$ anions and disordered [N(CH$_3$)$_4$]$^+$ cations.

- Hirshfeld surfaces and fingerprint plot were used to visualize and explore intermolecular interactions in the [N(CH$_3$)$_4$] [2,2'-Fe(1,7-*closo*-C$_2$B$_9$H$_{11}$)$_2$] crystal.